J. Phys. B: At. Mol. Opt. Phys. **30** (1997) 2199–2208. Printed in the UK PII: S0953-4075(97)80189-7

High-energy positronium formation in positron–hydrogenic ion collisions: scaling laws

O A Fojón†, R D Rivarola†, R Gayet‡, J Hanssen§ and P A Hervieux§

† Instituto de Física Rosario, CONICET-UNR and Escuela de Ciencias Exactas y Naturales, Facultad de Ciencias Exactas, Ingeniería y Agrimensura, Av. Pellegrini 250, 2000 Rosario, Argentina
‡ Centre de Physique Théorique et de Modélisations, Université de Bordeaux I, 351 cours de la Liberation, 33405 Talence, France
§ Laboratoire de Physique Moléculaire et des Collisions, Institut de Physique Rue Arago, Téchnopôle 2000, 57078 Metz Cedex 3, France

Received 9 December 1996, in final form 17 February 1997

Abstract. The electron capture process with the formation of positronium atoms in the ground state in collisions of high-energy positrons impacting on hydrogenic ions also in the ground state is studied theoretically. Contributions from double-step mechanisms in the collision process at high impact energies are discussed. Scaling laws for the theoretical differential and total cross sections valid at sufficiently high impact energies and nuclear charge of the target are obtained.

1. Introduction

During the last few years, a considerable amount of theoretical work has been devoted to the study of positronium formation by positron impact motivated by measurements obtained with the currently available high-intensity positron beams [1–8]. The theoretical work on the subject reveals that the positronium formation mechanism is not as fully understood as the charge transfer process by heavy projectiles. Only recently, positronium formation with ionic targets has been studied theoretically in a few works [9–11]. In one of these papers [11] (hereafter called I), the continuum distorted-wave final-state (CDW-FS) model was introduced to study the charge transfer process from the K-shell of a hydrogenic target to the K-shell of the positronium atom. In this model, distortions in the final channel related to the Coulomb continuum states of the positron and the electron in the field of the residual target are included. If no distortions are included in the final channel, the Coulomb Born approximation (CBA) [9] is obtained. Differential and total cross sections at intermediate impact energies for several hydrogenic targets have been obtained in I with the CDW-FS model employing a partial-wave technique. Also, CBA cross sections have been given. In this work, we focus on the impact of high-velocity positrons on hydrogenic targets. As the earlier technique becomes more slowly convergent as the impact energy increases, a new calculation scheme to evaluate the CDW-FS matrix elements is introduced. Following the work of Chen *et al* [12] as well as ideas from Roy *et al* [13] and Brauner *et al* [14], the CDW-FS matrix element is reduced and computed by means of numerical quadratures.

Atomic units are used unless otherwise specified.

0953-4075/97/092199+10$19.50

2. Theory

2.1. CBA and CDW-FS models

In this section, the CDW-FS and CBA models are briefly described. Let us consider the formation of positronium atoms in the ground state in a collision of a fast positron e^+ with a hydrogenic target T of nuclear charge Z_T also in the ground state. The geometrical parameters of the collision are given in figure 1.

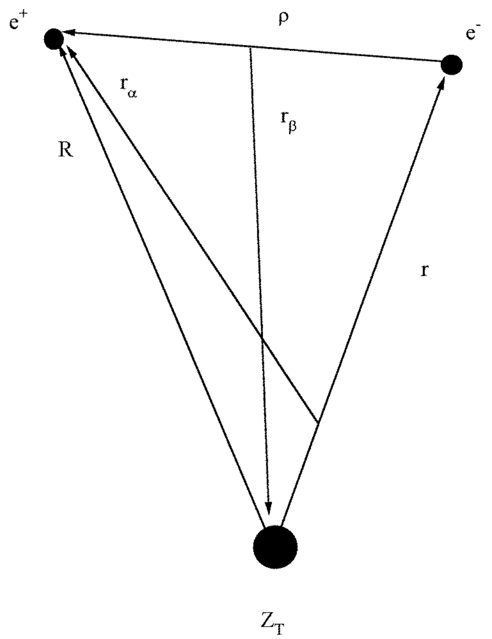

Figure 1. Coordinates used in the text.

The initial and final non-perturbed wavefunctions are given by

$$\Phi_\alpha = \varphi_i(\boldsymbol{r})\, \mathcal{F}^+_{\boldsymbol{k}_\alpha}(\boldsymbol{r}_\alpha) \tag{1}$$

$$\Phi_\beta = \varphi_f(\boldsymbol{\rho}) \exp(-\mathrm{i}\boldsymbol{k}_\beta \cdot \boldsymbol{r}_\beta) \tag{2}$$

where φ_i and φ_f are the initial and final bound wavefunctions. The function $\mathcal{F}^+_{\boldsymbol{k}_\alpha}(\boldsymbol{r}_\alpha)$ introduced in equation (1) is an outgoing Coulomb continuum wavefunction representing the positron moving in the field of an effective ion of charge $(Z_T - 1)$,

$$\mathcal{F}^+_{\boldsymbol{k}_\alpha}(\boldsymbol{r}_\alpha) = N^+_{\nu'_\alpha} \exp(\mathrm{i}\boldsymbol{k}_\alpha \cdot \boldsymbol{r}_\alpha)\, {}_1F_1(-\mathrm{i}\nu'_\alpha; 1; \mathrm{i}k_\alpha r_\alpha - \mathrm{i}\boldsymbol{k}_\alpha \cdot \boldsymbol{r}_\alpha) \tag{3}$$

with

$$\nu'_\alpha = (Z_T - 1)\frac{\mu_\alpha}{k_\alpha} = \frac{(Z_T - 1)}{v} \tag{4}$$

$$N^+_{\nu'_\alpha} = \Gamma(1 + \mathrm{i}\nu'_\alpha) \exp\left(-\tfrac{1}{2}\pi \nu'_\alpha\right). \tag{5}$$

The *prior* version of the CDW-FS matrix element reads [11]

$$\begin{aligned} T^{-,\text{CDW-FS}}_{\alpha\beta} = N^+_{\nu'_\alpha}\, N^{-*}_{\beta_+}\, N^{-*}_{\beta_-} \int \mathrm{d}\boldsymbol{R}\, \mathrm{d}\boldsymbol{r} \exp\left\{\mathrm{i}\boldsymbol{k}_\alpha \cdot \boldsymbol{R} + \mathrm{i}\boldsymbol{k}_\beta \cdot \boldsymbol{r}_\beta\right\} \varphi^*_f(\boldsymbol{\rho}) \\ \times \left(\frac{1}{R} - \frac{1}{\rho}\right) {}_1F_1(-\mathrm{i}\beta_+; 1; \mathrm{i}\boldsymbol{v}_\beta \cdot \boldsymbol{R} + \mathrm{i}v_\beta R) \\ \times\, {}_1F_1(\mathrm{i}\beta_-; 1; \mathrm{i}\boldsymbol{v}_\beta \cdot \boldsymbol{r} + \mathrm{i}v_\beta r)\, \varphi_i(\boldsymbol{r})\, {}_1F_1(-\mathrm{i}\nu'_\alpha; 1; \mathrm{i}k_\alpha R - \mathrm{i}\boldsymbol{k}_\alpha \cdot \boldsymbol{R}) \end{aligned} \tag{6}$$

where the approximation $\boldsymbol{r}_\alpha \simeq \boldsymbol{R}$ has been made. $\boldsymbol{k}_\alpha$ and $\boldsymbol{k}_\beta$ are the wavevectors for the reduced positron in the entry channel and for the reduced positronium in the final channel, respectively. Moreover, we have defined

$$\boldsymbol{v}_\beta = \frac{\boldsymbol{k}_\beta}{\mu_\beta} \tag{7}$$

and

$$\beta_+ \simeq \beta_- \simeq \beta = \frac{Z_T}{v_\beta} \tag{8}$$

$$N^-_{\beta_\pm} = \Gamma(1 \mp \mathrm{i}\beta_\pm)\exp(\mp\tfrac{1}{2}\pi\beta_\pm)\,. \tag{9}$$

Setting $\beta_+ = \beta_- = \beta = 0$ in the CDW-FS matrix element, the CBA [9] matrix element is obtained.

Finally, DCS and TCS are obtained by using

$$\frac{\mathrm{d}\sigma}{\mathrm{d}\Omega} = \frac{1}{4\pi^2}\,\frac{k_\beta}{k_\alpha}\mu_\alpha\mu_\beta|T_{\alpha\beta}|^2 \tag{10}$$

and

$$\sigma = \int \mathrm{d}\Omega\,(\mathrm{d}\sigma/\mathrm{d}\Omega) \tag{11}$$

respectively.

2.2. *Evaluation of the CDW-FS matrix element*

In I, a partial-wave technique has been employed to evaluate the CDW-FS matrix element. As the impact energy increases, higher values of angular orbital momenta are required and more computer time is required to achieve convergence. As the aim of this work is to study the impact of high-velocity positrons, a new calculation scheme which is more efficient than the early one is introduced.

Let us consider the CDW-FS matrix element given by equation (6). Firstly, the confluent hypergeometric function depending on ν'_α is developed as [15]

$${}_1F_1(-\mathrm{i}\nu'_\alpha;1;\mathrm{i}k_\alpha R - \mathrm{i}\boldsymbol{k}_\alpha\cdot\boldsymbol{R}) = -(2\pi\mathrm{i})^{-1}\int_1^{(0^+)}\mathrm{d}u\;(-u)^{-\mathrm{i}\nu'_\alpha-1}\;(1-u)^{\mathrm{i}\nu'_\alpha}\mathrm{e}^{\mathrm{i}(k_\alpha R - \mathrm{i}\boldsymbol{k}_\alpha\cdot\boldsymbol{R})u}\,. \tag{12}$$

Inserting the integral representation (12) in the CDW-FS matrix element given by equation (6), we obtain

$$T^{-,\mathrm{CDW\text{-}FS}}_{\alpha\beta} = -K(2\pi\mathrm{i})^{-1}\int_1^{(0^+)}\mathrm{d}u(-u)^{-\mathrm{i}\nu'_\alpha-1}(1-u)^{\mathrm{i}\nu'_\alpha}J(u) \tag{13}$$

with K

$$K = \frac{Z_T^{3/2}}{2\sqrt{2\pi}}N^+_{\nu'_\alpha}N^{-*}_{\beta_+}N^{-*}_{\beta_-} \tag{14}$$

and where $J(u)$ is given by

$$\begin{aligned} J(u) = \int \mathrm{d}\boldsymbol{R}\,\mathrm{d}\boldsymbol{r}\exp\{\mathrm{i}\boldsymbol{M}\cdot\boldsymbol{R} + \mathrm{i}vuR\}\left(\frac{1}{R}-\frac{1}{\rho}\right) \\ \times {}_1F_1(-\mathrm{i}\beta_+;1;\mathrm{i}\boldsymbol{v}_\beta\cdot\boldsymbol{R}+\mathrm{i}v_\beta R)\,{}_1F_1(\mathrm{i}\beta_-;1;\mathrm{i}\boldsymbol{v}_\beta\cdot\boldsymbol{r}+\mathrm{i}v_\beta r) \\ \times\exp(-\mathrm{i}\boldsymbol{v}_\beta\cdot\boldsymbol{r} - Z_T r)\exp(-\rho/2) \end{aligned} \tag{15}$$

with

$$\boldsymbol{M} = \boldsymbol{v}(1-u) - \boldsymbol{v}_\beta \,. \tag{16}$$

In obtaining $J(u)$, the approximation $\boldsymbol{k}_\alpha \simeq \boldsymbol{v}$ has been made.

Secondly, and using the technique described in [12], the CDW-FS matrix element may be written as

$$\begin{aligned} T_{\alpha\beta}^{-,\text{CDW-FS}} &= -K \left\{ J(u=0) + \frac{\sinh(\pi\nu'_\alpha)}{\pi \mathrm{i}} \int_0^1 \mathrm{d}u \left(\frac{1-u}{u}\right)^{\mathrm{i}\nu'_\alpha} \frac{[J(u) - J(u=0)]}{u} \right\} \\ &= -K \left\{ J(u=0) + \frac{\sinh(\pi\nu'_\alpha)}{\pi \mathrm{i}} \int_{-\infty}^{+\infty} \mathrm{d}y \frac{\mathrm{e}^{(1+\mathrm{i}\nu'_\alpha)y}}{1+\mathrm{e}^y} [J(u) - J(u=0)] \right\} \end{aligned} \tag{17}$$

with $u = (1+\mathrm{e}^y)^{-1}$.

Thirdly, the integral $J(u)$ is studied. This kind of integral has been analysed in [12] and reduced to a two-dimensional integral with the aid of parametric derivatives. Then, introducing the parameters λ_i with $i = 1, 2, 3$, the following integral is defined:

$$\begin{aligned} J(\lambda_1, \lambda_2, \lambda_3, \boldsymbol{P}_1, \boldsymbol{P}_2, \boldsymbol{K}_1, \boldsymbol{K}_2; u) &= \left(\frac{\partial^2}{\partial\lambda_3\,\partial\lambda_2} - \frac{\partial^2}{\partial\lambda_1\,\partial\lambda_2}\right) \int \mathrm{d}\boldsymbol{R}\,\mathrm{d}\boldsymbol{r} \exp\{-\mathrm{i}\boldsymbol{P}_1\cdot\boldsymbol{R}\} \frac{\mathrm{e}^{-\lambda_1 R}}{R} \\ &\quad \times {}_1F_1(-\mathrm{i}\beta_+; 1; \mathrm{i}[K_1 R - \boldsymbol{K}_1\cdot\boldsymbol{R}]) \exp\{-\mathrm{i}\boldsymbol{P}_2\cdot\boldsymbol{r}\} \frac{\mathrm{e}^{-\lambda_2 r}}{r} \\ &\quad \times {}_1F_1(\mathrm{i}\beta_-; 1; \mathrm{i}[K_2 r - \boldsymbol{K}_2\cdot\boldsymbol{r}]) \frac{\mathrm{e}^{-\lambda_3\rho}}{\rho} \end{aligned} \tag{18}$$

where $J(u)$ is obtained by making

$$\boldsymbol{P}_1 = -\boldsymbol{M} \qquad \boldsymbol{P}_2 = \boldsymbol{v}_\beta \tag{19}$$

$$\boldsymbol{K}_1 = -\boldsymbol{v}_\beta \qquad \boldsymbol{K}_2 = -\boldsymbol{v}_\beta \tag{20}$$

and taking after derivation

$$\lambda_1 = \epsilon - \mathrm{i}uv \qquad \lambda_2 = Z_T \qquad \lambda_3 = \tfrac{1}{2}\,. \tag{21}$$

At the end of the calculations, $\epsilon = 0$ must be taken.

Using the results of Chen [12], one obtains

$$\begin{aligned} &J(\lambda_1, \lambda_2, \lambda_3, \boldsymbol{P}_1, \boldsymbol{P}_2, \boldsymbol{K}_1, \boldsymbol{K}_2; u) \\ &\quad = N(t=0) + \frac{\sinh(\pi\beta_+)}{\pi \mathrm{i}} \int_{-\infty}^{+\infty} \mathrm{d}x \frac{\mathrm{e}^{(1+\mathrm{i}\beta_+)x}}{1+\mathrm{e}^x} [N(t) - N(t=0)] \end{aligned} \tag{22}$$

with $t = (1+\mathrm{e}^x)^{-1}$. The function $N(t)$ reads

$$N(t) = 16\pi^2 \int_0^\infty \mathrm{d}s \left(\frac{\partial^2}{\partial\lambda_3\,\partial\lambda_2} - \frac{\partial^2}{\partial\lambda_1\,\partial\lambda_2}\right) \left[\frac{1}{\epsilon_0} \left(1 + \frac{\epsilon_1}{\epsilon_0}\right)^{-\mathrm{i}\beta_-}\right] \tag{23}$$

where

$$\begin{aligned} \epsilon_0 = &\left\{(\boldsymbol{P}_1 + \boldsymbol{P}_2)^2 + (\lambda_1+\lambda_2)^2 + 2[(\boldsymbol{P}_1+\boldsymbol{P}_2)\cdot\boldsymbol{K}_1 - \mathrm{i}(\lambda_1+\lambda_2)K_1]t\right\} \\ &\times (s^2 + 2\lambda_3 s) + 2s[\gamma_1(\lambda_3^2 + P_2^2 + \lambda_2^2) + \lambda_2(\lambda_3^2 + q_1^2 + \gamma_1^2)] \\ &+ [(\gamma_1+\lambda_3)^2 + q_1^2]\,[(\lambda_2+\lambda_3)^2 + P_2^2] \end{aligned} \tag{24}$$

$$\begin{aligned} \epsilon_1 = &\,2\,[(\boldsymbol{P}_1+\boldsymbol{P}_2)\cdot\boldsymbol{K}_2 - \mathrm{i}(\lambda_1+\lambda_2)K_2 + (\boldsymbol{K}_1\cdot\boldsymbol{K}_2 - K_1K_2)\,t]\,(s^2 + 2\lambda_3 s) \\ &+ 2s[2\gamma_1(\boldsymbol{P}_2\cdot\boldsymbol{K}_2 - \mathrm{i}\lambda_2 K_2) - \mathrm{i}K_2(\lambda_3^2 + q_1^2 + \gamma_1^2)] \\ &+ 2[(\gamma_1+\lambda_3)^2 + q_1^2][\boldsymbol{P}_2\cdot\boldsymbol{K}_2 - \mathrm{i}(\lambda_2+\lambda_3)\,K_2] \end{aligned} \tag{25}$$

with

$$\boldsymbol{q}_1 = \boldsymbol{P}_1 + \boldsymbol{K}_1 t \qquad \gamma_1 = \lambda_1 - K_1 t\,. \tag{26}$$

2.3. Scaling laws

In this section, scaling laws for the CDW-FS and CBA differential and total cross sections are derived. These scaling laws are valid when the impact energy and the nuclear charge of the target are sufficiently high.

Fourier transforming the positronium bound state and using relations between coordinates, the CDW-FS matrix element may be expressed as

$$T_{\alpha\beta}^{-,\text{CDW-FS}} = N_{\nu'_\alpha}^{+} N_{\beta_+}^{-*} N_{\beta_-}^{-*} N_{\text{Ps}} \int \mathrm{d}\Omega_\tau \, \mathrm{d}\tau \, \frac{\tau^2}{\left(\tau^2 + \frac{1}{4}\right)^2} \int \mathrm{d}\boldsymbol{R}\, \mathrm{d}\boldsymbol{r} \; I(\boldsymbol{R}, \boldsymbol{r}, \boldsymbol{\tau}) \tag{27}$$

with

$$I(\boldsymbol{R}, \boldsymbol{r}, \boldsymbol{\tau}) = \mathrm{e}^{\mathrm{i}\left(\boldsymbol{k}_\alpha - \frac{1}{2}\boldsymbol{k}_\beta + \boldsymbol{\tau}\right)\cdot \boldsymbol{\rho}} \; K(\boldsymbol{R}, \boldsymbol{r}) \qquad N_{\text{Ps}} = \frac{1}{4\pi^2\sqrt{2}\pi} \tag{28}$$

and where

$$\begin{aligned} K(\boldsymbol{R}, \boldsymbol{r}) = \mathrm{e}^{\mathrm{i}(\boldsymbol{k}_\alpha - \boldsymbol{k}_\beta)\cdot \boldsymbol{r}} &\left(\frac{1}{R} - \frac{1}{\rho}\right) {}_1F_1(-\mathrm{i}\beta_+; 1; \mathrm{i}\boldsymbol{v}_\beta \cdot \boldsymbol{R} + \mathrm{i}v_\beta R) \\ &\times {}_1F_1(\mathrm{i}\beta_-; 1; \mathrm{i}\boldsymbol{v}_\beta \cdot \boldsymbol{r} + \mathrm{i}v_\beta r)\varphi_i(\boldsymbol{r}) \\ &\times {}_1F_1(-\mathrm{i}\nu'_\alpha; 1; \mathrm{i}k_\alpha R - \mathrm{i}\boldsymbol{k}_\alpha \cdot \boldsymbol{R})\,. \end{aligned} \tag{29}$$

In equation (27), the expression $\tau^2(\tau^2 + \frac{1}{4})^{-2}$ is highly peaked around $\tau_0 = \frac{1}{2}$. Therefore, the most important contribution of $I(\boldsymbol{R}, \boldsymbol{r}, \boldsymbol{\tau})$ to the τ-integration comes from the region around $\boldsymbol{\tau} = \tau_0 \hat{\tau}$ with $\hat{\tau} = \boldsymbol{\tau}/|\boldsymbol{\tau}|$. Then, if $\boldsymbol{k}_\alpha$ and $\boldsymbol{k}_\beta$ are such that

$$\left|\boldsymbol{k}_\alpha - \tfrac{1}{2}\boldsymbol{k}_\beta\right| \gg \tfrac{1}{2} \tag{30}$$

it is valid to write

$$\begin{aligned} T_{\alpha\beta}^{-,\text{CDW-FS}} \simeq N_{\nu'_\alpha}^{+} N_{\beta_+}^{-*} N_{\beta_-}^{-*} N_{\text{Ps}} &\left[\int \mathrm{d}\Omega_\tau \, \mathrm{d}\tau \, \frac{\tau^2}{(\tau^2 + \frac{1}{4})^2}\right] \\ &\times \int \mathrm{d}\boldsymbol{R}\, \mathrm{d}\boldsymbol{r} \exp\left\{\mathrm{i}\left(\boldsymbol{k}_\alpha \cdot \boldsymbol{R} + \boldsymbol{k}_\beta \cdot \boldsymbol{r}_\beta\right)\right\} \\ &\times \left(\frac{1}{R} - \frac{1}{\rho}\right) {}_1F_1(-\mathrm{i}\beta_+; 1; \mathrm{i}\boldsymbol{v}_\beta \cdot \boldsymbol{R} + \mathrm{i}v_\beta R) \\ &\times {}_1F_1(\mathrm{i}\beta_-; 1; \mathrm{i}\boldsymbol{v}_\beta \cdot \boldsymbol{r} + \mathrm{i}v_\beta r)\varphi_i(\boldsymbol{r}) \\ &\times {}_1F_1(-\mathrm{i}\nu'_\alpha; 1; \mathrm{i}k_\alpha R - \mathrm{i}\boldsymbol{k}_\alpha \cdot \boldsymbol{R})\,. \end{aligned} \tag{31}$$

Let us consider the following scaling in the impact energy:

$$E_i^{(Z_{T_2})} = \left(\frac{Z_{T_2}}{Z_{T_1}}\right)^2 E_i^{(Z_{T_1})} \tag{32}$$

which is equivalent to

$$\boldsymbol{k}_\alpha^{(Z_{T_2})} = \left(\frac{Z_{T_2}}{Z_{T_1}}\right) \boldsymbol{k}_\alpha^{(Z_{T_1})}\,. \tag{33}$$

The upper indices indicate that the magnitudes involved are the ones corresponding to a collision of a positron on a target of nuclear charge Z_T. From the energy conservation law, it follows that

$$k_\beta^{(Z_{T_2})} = (Z_{T_2}/Z_{T_1}) \left\{ 1 - \frac{1}{4E_i^{(Z_{T_1})} - 2Z_{T_1}^2 + 1} \left[1 - \left(\frac{Z_{T_1}}{Z_{T_2}} \right)^2 \right] \right\}^{1/2} k_\beta^{(Z_{T_1})} \tag{34}$$

where use has been made of the binding energy of a hydrogenic atom of charge Z_T. Equation (34) reveals that the scaling in final momenta is only approximately true. However, as E_i increases the scaling in momentum k_β becomes more and more valid.

The Sommerfeld parameters β_+ and β_- are almost invariant with respect to the scaling in momenta, i.e.

$$\beta_j^{(Z_{T_1})} \simeq \beta_j^{(Z_{T_2})} \tag{35}$$

with $j = +, -$. In contrast, the Sommerfeld parameter ν'_α does not behave like the β_j parameters. However, at a fixed impact energy $E_i^{(Z_T)}$ their scaling improves as Z_T increases. For Z_T fixed, the scaling improves as E_i increases. A similar analysis leads to the same conclusions with respect to the normalization constants $N_{\beta_+}^-$, $N_{\beta_-}^-$ and $N_{\nu'_\alpha}^+$.

Let us now consider the following scaling for the independent coordinates:

$$\boldsymbol{r}^{(Z_{T_2})} = \left(\frac{Z_{T_1}}{Z_{T_2}} \right) \boldsymbol{r}^{(Z_{T_1})} \tag{36}$$

$$\boldsymbol{R}^{(Z_{T_2})} = \left(\frac{Z_{T_1}}{Z_{T_2}} \right) \boldsymbol{R}^{(Z_{T_1})} . \tag{37}$$

As a consequence, the coordinate $\boldsymbol{\rho}$ transforms as

$$\boldsymbol{\rho}^{(Z_{T_2})} = \left(\frac{Z_{T_1}}{Z_{T_2}} \right) \boldsymbol{\rho}^{(Z_{T_1})} . \tag{38}$$

Plane-wave functions, initial bound state and confluent hypergeometric functions depending on β_+ and β_- all remain unaltered after the transformations. Of course, this is only true in an approximate way for the hypergeometric function depending on ν'_α according to the facts already discussed. The higher the impact energy and the nuclear charge of the target, the better the approximation.

Now by using the scaling in momenta and coordinates, the following relation:

$$T_{\alpha\beta}^{-,\text{CDW-FS}}(Z_{T_2}, E_i^{(Z_{T_2})}) \simeq \left(\frac{Z_{T_1}}{Z_{T_2}} \right)^{7/2} T_{\alpha\beta}^{-,\text{CDW-FS}}\left(Z_{T_1}, E_i^{(Z_{T_2})} \left(\frac{Z_{T_1}}{Z_{T_2}} \right)^2 \right) \tag{39}$$

holds for sufficiently high impact energy and Z_T. This is the scaling law for the CDW-FS matrix elements. As the CBA matrix elements are easily obtained from the CDW-FS ones by making $\beta_+ = \beta_- = 0$, the CBA matrix elements verify exactly the same scaling law.

According to equations (10) and (11), CDW-FS and CBA differential and total cross sections verify the following relations:

$$\frac{\mathrm{d}\sigma}{\mathrm{d}\Omega}(Z_{T_2}, E_i^{(Z_{T_2})}) \simeq \left(\frac{Z_{T_1}}{Z_{T_2}} \right)^7 \frac{\mathrm{d}\sigma}{\mathrm{d}\Omega}\left(Z_{T_1}, E_i^{(Z_{T_2})} \left(\frac{Z_{T_1}}{Z_{T_2}} \right)^2 \right) \tag{40}$$

$$\sigma(Z_{T_2}, E_i^{(Z_{T_2})}) \simeq \left(\frac{Z_{T_1}}{Z_{T_2}} \right)^7 \sigma\left(Z_{T_1}, E_i^{(Z_{T_2})} \left(\frac{Z_{T_1}}{Z_{T_2}} \right)^2 \right) . \tag{41}$$

Moreover, as the scaling factor is the same for both the CDW-FS and CBA approximations, the following relation also holds:

$$\frac{\sigma(Z_{T_2}, E_i^{(Z_{T_2})})_{\text{CDW-FS}}}{\sigma(Z_{T_1}, E_i^{(Z_{T_2})}\left(Z_{T_1}/Z_{T_2}\right)^2)_{\text{CDW-FS}}} \simeq \frac{\sigma(Z_{T_2}, E_i^{(Z_{T_2})})_{\text{CBA}}}{\sigma(Z_{T_1}, E_i^{(Z_{T_2})}\left(Z_{T_1}/Z_{T_2}\right)^2)_{\text{CBA}}}. \tag{42}$$

A similar relation for the differential cross sections is also valid. In general, CBA differential and total cross sections are more easily computed than the corresponding CDW-FS ones.

3. Results

A discussion on the contribution of the Thomas two-step mechanisms to the cross section has already been given in I. Here, the presence of the Thomas peak in the DCS is discussed at intermediate and high impact energies. In figures 2(*a*) and (*b*), CBA and CDW-FS DCS as a function of the ejection angle of the positronium atom for $e^+ + He^+$ at impact energy $E_i = 2$ and 10 keV, respectively, are shown. In the last case, relativistic effects are not taken into account despite their possible importance. In the CBA DCS no Thomas peak is observed as expected from a first-order Born theory. In contrast, in the CDW-FS DCS

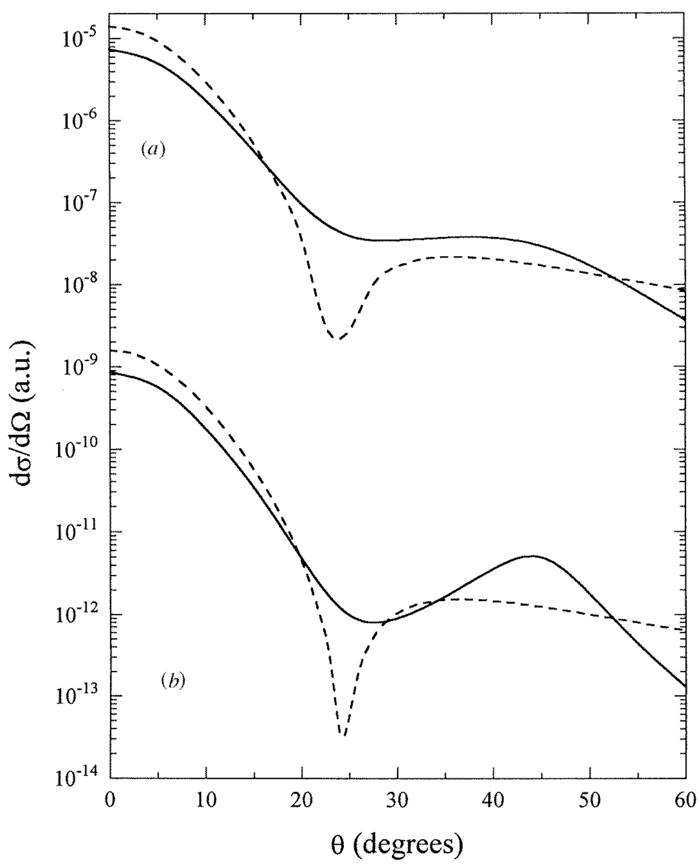

Figure 2. CDW-FS (——) and CBA (– – –) DCS for $e^+ + He^+$. (*a*) Impact energy $E_i = 2$ keV. (*b*) $E_i = 10$ keV.

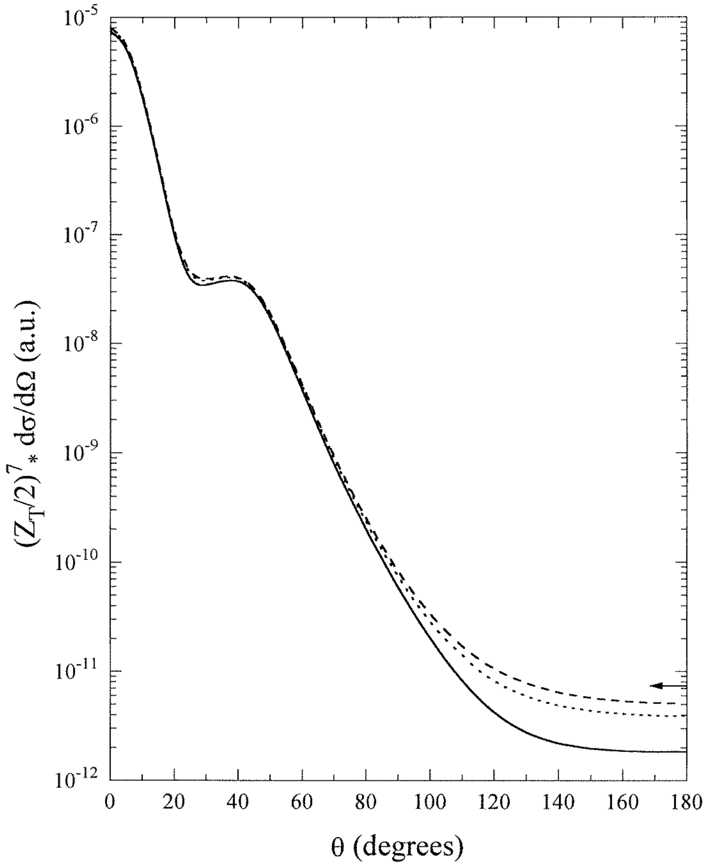

Figure 3. CDW-FS scaled DCS with respect to He^+. ——, $Z_T = 2$ and $E_i = 2$ keV; . . . , $Z_T = 3$ and $E_i = 4.5$ keV; – – –, $Z_T = 4$ and $E_i = 8$ keV; ←, $Z_T = 10$ and $E_i = 50$ keV at $\theta = 180°$.

Table 1. Scaled TCS CDW-FS. $x[y]$ represents $\times 10^y$.

E_i (eV)	He^+	Li^{2+}	Be^{3+}	B^{4+}
500	5.4[−4]	5.7[−4]	5.9[−4]	6.2[−4]
1 000	2.0[−5]	2.0[−5]	2.0[−5]	2.0[−5]
2 000	5.7[−7]	6.2[−7]	6.3[−7]	6.1[−7]
5 000	3.5[−9]	3.6[−9]	3.7[−9]	3.8[−9]
10 000	6.5[−11]	6.9[−11]	7.2[−11]	7.6[−11]

a distinct peak is observed at $\theta \simeq 45°$, particularly at 10 keV. Present CDW-FS DCS at 2 keV agree with the previous ones given in I. However, the additional structures around and beyond the Thomas' peak have now disappeared. They may be attributed to a precision problem in the partial-wave method employed in I. It may be verified that the contribution of the peak to the total cross sections even at very high impact energy is not as important as in the case of heavy ion impact. Finally, the differences between the CDW-FS and CBA results over the entire angular domain give an indication of the contribution of the higher orders of CDW-FS.

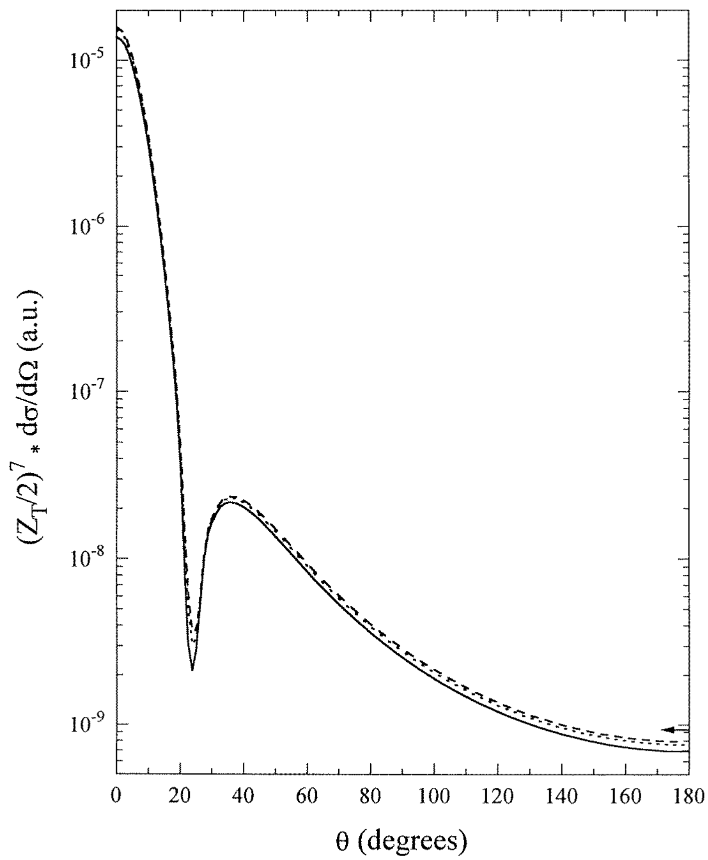

Figure 4. Same as figure 3 but for CBA DCS.

Table 2. Same as table 1 but for CBA.

E_i (eV)	He^+	Li^{2+}	Be^{3+}	B^{4+}
500	9.8[−4]	1.2[−3]	1.3[−3]	1.4[−3]
1 000	4.0[−5]	4.0[−5]	4.0[−5]	4.6[−5]
2 000	9.3[−7]	1.0 [-6]	1.1[−6]	1.1[−6]
5 000	5.6[−9]	5.9 [-9]	6.0[−9]	6.1[−9]
10 000	1.0[−10]	1.1 [-10]	1.1[−10]	1.1[−10]

In figures 3 and 4, CDW-FS and CBA scaled differential cross sections (SDCS) with respect to He^+ for the system $e^+ + (Z_T + e^-)$ ($Z_T = 2, 3, 4$) are shown. The arrow indicates the SDCS value for $Z_T = 10$ and $\theta = 180^\circ$. It can be seen that the scaling law is very good. Small deviations from the scaling are observed at large scattering angles but as Z_T increases the scaling improves. As the TCS are dominated by the small angular region, good agreement is also expected for the scaled TCS (STCS). In tables 1 and 2, CDW-FS and CBA STCS, respectively, with respect to He^+ are shown for the systems already mentioned. Again, the scaling law is very good.

Acknowledgments

The authors would like to thank the CNUSC (Centre National Universitaire Sud de Calcul) for providing free computer time. OAF and RDR also gratefully acknowledge support from the University of Metz within the framework of the collaboration with the University of Rosario.

References

[1] McGuire J H, Sil N C and Deb N C 1986 *Phys. Rev.* A **34** 685
Deb N C, McGuire J H and Sil N C 1987 *Phys. Rev.* A **35** 3707
[2] Basu M and Ghosh A S 1988 *J. Phys. B: At. Mol. Opt. Phys.* **21** 3439
[3] Roberts M J 1989 *J. Phys. B: At. Mol. Opt. Phys.* **22** 3315
[4] Mandal C R, Mandal Mita and Mukherjee S C 1991 *Phys. Rev.* A **44** 2968
[5] Igarashi A and Toshima N 1993 *Phys. Rev.* A **47** 2386
[6] Ward S J and Macek J H 1994 *Hyperfine Interactions* **89** 477
[7] Bransden B H and Noble J C 1994 *Adv. At. Mol. Opt. Phys.* **32** 19
[8] Laricchia G 1995 *Proc. 19th Int. Conf. on Physics of Electronic and Atomic Collisions (Whistler)* Book of contributed papers p 385
[9] Fojón O A, Gayet R, Hanssen J and Rivarola R D 1995 *Phys. Scr.* **51** 204
Fojón O A, Gayet R, Hanssen J and Rivarola R D 1995 *Phys. Scr.* **52** 607
[10] Gianturco F A and Melissa R 1996 *J. Phys. B: At. Mol. Opt. Phys.* **29** L719
[11] Fojón O A, Gayet R, Hervieux P A, Hanssen J and Rivarola R D 1996 *Phys. Rev.* A **54** 4923
[12] Chen X J, Wen B, Xu Y W and Zheng Y Y 1992 *J. Phys. B: At. Mol. Opt. Phys.* **25** 4661
[13] Roy A, Roy K and Sil N C 1980 *J. Phys. B: At. Mol. Phys.* **13** 3443
[14] Brauner M, Briggs J S and Klar H 1989 *J. Phys. B: At. Mol. Opt. Phys.* **22** 2265
[15] Landau L D and Lifschitz E M 1977 *Quantum Mechanics Non-relativistic Theory* (New York: Pergamon)